Cl^- Concentration Dependence of Photovoltage Generation by Halorhodopsin from *Halobacterium salinarum*

Eiro Muneyuki,* Chie Shibazaki,† Yoichiro Wada,† Manabu Yakushizin,† and Hiroyuki Ohtani†

*Chemical Resources Laboratory (Research Laboratory of Resources Utilization), Tokyo Institute of Technology, Yokohama 226-8503, and †Department of Biomolecular Engineering, Graduate School of Bioscience and Biotechnology, Tokyo Institute of Technology, Yokohama 226-8501, Japan

ABSTRACT The photovoltage generation by halorhodopsin from *Halobacterium salinarum* (shR) was examined by adsorbing shR-containing membranes onto a thin polymer film. The photovoltage consisted of two major components: one with a sub-millisecond range time constant and the other with a millisecond range time constant with different amplitudes, as previously reported. These components exhibited different Cl^- concentration dependencies (0.1–9 M). We found that the time constant for the fast component was relatively independent of the Cl^- concentration, whereas the time constant for the slow component increased sigmoidally at higher Cl^- concentrations. The fast and the slow processes were attributed to charge (Cl^-) movements within the protein and related to Cl^- ejection, respectively. The laser photolysis studies of shR-membrane suspensions revealed that they corresponded to the formation and the decay of the N intermediate. The photovoltage amplitude of the slow component exhibited a distorted bell-shaped Cl^- concentration dependence, and the Cl^- concentration dependence of its time constant suggested a weak and highly cooperative Cl^--binding site(s) on the cytoplasmic side (apparent K_D of ~5 M and Hill coefficient ≥5). The Cl^- concentration dependence of the photovoltage amplitude and the time constant for the slow process suggested a competition between spontaneous relaxation and ion translocation. The time constant for the relaxation was estimated to be >100 ms.

INTRODUCTION

Halorhodopsin (hR) is a light-driven chloride pump in the cell membranes of halobacteria that transports Cl^- into the cells. This Cl^- pump is analogous to the light-driven proton pump, bacteriorhodopsin (bR), which is well studied in structure and function (Stoeckenius, 1999). Photoisomerization of the all-*trans* retinal to the 13-*cis* form triggers ion translocation in both hR and bR. However, they translocate different ions (Cl^- for hR and protons for bR) in different directions (inward for hR and outward for bR). Elucidation of the ion translocation mechanisms of both proteins will provide insights into the general principle that determines specificity and vectoriality of ion translocation.

Among the numerous hRs reported (Ihara et al., 1999; Otomo et al., 1992; Soppa et al., 1993), hR from *Halobacterium salinarum* (shR) and hR from *Natronobacterium pharaonis* (phR) have been most extensively studied. Compared with bR, however, details of the mechanisms of hR function are still unclear. Though the molecular structure of shR was recently reported (Kolbe et al., 2000), only the Cl^- bound near the protonated Schiff base was seen in the structure. Other Cl^--binding sites, presumably with low affinity (Okuno et al., 1999), were not observed, and the precise pathway of Cl^- translocation is still unclear. The photocycle scheme of hR is also still a matter of debate. Different researchers apply different nomenclature to the photointermediates. In spectral and kinetic analogy to the intermediates of bR, Váró et al. identified HR, K, L, N, O, and HR′ in the phR photocycle (Váró et al., 1995a,b) and HR, K, L1, L2, and N intermediates for shR (Váró et al., 1995c). Here, K, L, N, and O intermediates have absorption maxima around 600, 520, 580, and 640 nm, respectively. The K, L, and O intermediates seem to correspond, respectively, to the HR600, HR520 (I and II), and HR640 named by others (Ames et al., 1992; Oesterhelt 1995). Based on transient visible spectroscopy on the nanosecond time scale (Zimányi et al., 1989) and Fourier transform infrared spectroscopy (Hutson et al., 2001), two substates for the K intermediate were suggested. In this manuscript, we adopt the nomenclature used by Váró et al. (1995a,b,c). The formation and the decay of the O (or HR640) intermediate in shR were assigned as Cl^- release and uptake, respectively, by Ames et al. (1992) for shR. But the O intermediate of shR was proposed to originate in the 13-*cis* photocycle and/or the photocycle of the Cl^--free form (Váró et al., 1995c). Rüdiger and Oesterhelt (1997) suggested that the apparent absence of O in the Cl^--transporting photocycle of shR reflects some experimental conditions that can affect its spectroscopic detection. On the other hand, Kalaidzidis et al. (1998) excluded the O intermediate even from phR photocycle. Consequently, the ambiguity in the assignment of the Cl^--translocating steps in the photocycle is greater than ever.

Previously, we examined the photocurrent and photovoltage generation by shR and phR by adsorbing hR-containing membranes onto a thin polymer film. Time-resolved photovoltage measurements revealed that the photovoltage consisted of two major components: one with a sub-millisecond

Submitted November 13, 2001, and accepted for publication May 30, 2002.

Address reprint requests to Dr. Eiro Muneyuki, Tokyo Institute of Technology, Nagatsuta 4259, Midori-ku, Yokohama 226-8503, Japan. Tel.: 045-924-5232; Fax: 045-924-5277; E-mail: emuneyuk@res.titech.ac.jp.

0006-3495/02/10/1749/11 $2.00

range time constant and the other with a millisecond range time constant with different amplitudes. We concluded that the former and the latter corresponded to the N intermediate formation and decay, respectively (Muneyuki et al., 1999). This conclusion has recently been confirmed by others (Ludmann et al., 2000). However, it was not necessarily clear whether the two steps corresponded to Cl^- uptake from the medium, Cl^- release to the medium, or Cl^- translocation within the protein molecule. Thus, the next step toward an understanding of the Cl^- transport mechanism by halorhodopsin is the characterization of these electrogenic processes. In the present study, we examined the time-resolved photovoltage generation by shR over a wide Cl^- concentration range (0.1–9 M) and found a characteristic Cl^- concentration dependence of the time constant for the electrogenic processes. Based on the present results, we discuss the nature of the electrogenic processes in relation to the Cl^- movement within and Cl^- release from the protein. Furthermore, we found a novel relationship between the amplitude of photovoltage and the associated time constant, which depends on Cl^- concentrations. We propose that the Cl^- concentration dependence of the time constant and amplitude reflects a competition between spontaneous relaxation and ion translocation.

MATERIALS AND METHODS

Materials

The membrane fragments containing shR were kind gifts from Dr. R. Needleman (Wayne State University). The membranes were further purified by sucrose density gradient centrifugation (Oesterhelt and Stoeckenius, 1974). The shR-overproduced membranes were suspended in 20 mM Tris-maleate buffer containing 4 M NaCl and 2 mM $MgCl_2$ (pH 7.0).

Setup for electrical measurement

The experimental system was the same as described previously (Muneyuki et al., 1999). The system consists of a chamber connected to a specially designed high-input impedance amplifier with light-shielded Ag-AgCl electrodes and a laser flash system that is triggered by a personal computer. A 0.9-μm-thick polyester film (Lumirror, Toray Industries, Tokyo, Japan), to which membrane fragments were adsorbed, was placed between two compartments in the chamber. The Nd-YAG laser (532 nm; Surelite I-10, Continuum, Santa Clara, CA) was triggered by a personal computer equipped with a high-speed AD converter (2 MHz at maximum; model EC2372A-1, Elmec, Tokyo, Japan). The data were collected every 1 μs and stored on removable media of the personal computer.

Adsorption of membrane fragments and photovoltage measurement

The adsorption of the shR-overproduced membranes to the film was carried out as described previously (Muneyuki et al., 1998). Briefly, 60–80 μl of the membrane suspension was directly applied on one side of the polyester film in the chamber and was incubated for >40 min at room temperature. Excess membranes were removed by pipette, and 1.5 ml of a buffer containing 50 mM Tris-maleate (pH 7.0) and appropriate salts (typically, 0.5 or 1.5 M $CaCl_2$ or 1 or 3 M NaCl) was filled in both compartments. The buffer in the compartment on the membrane-adsorbed side was exchanged twice with the same buffer to wash out residual unbound membranes. Subsequently, 75 μl of 10% octylglucoside solution was added and incubated for ~1 min. The chamber was washed several times and filled with the buffer containing the desired concentration of salts.

Photovoltage measurements of the shR were carried out at room temperature using 50 mM Tris-maleate (pH 7.0) containing various kinds of salts. Photoexcitation was carried out at 532 nm with the Nd-YAG laser, and the data were stored as described above.

Photochemical cycle measurements

The main configuration of the laser flash photolysis apparatus has been described elsewhere (Ohtani et al., 1994). Membrane suspensions (1-cm light pass) were excited by a second harmonic (532 nm) of a Q-switched Nd-YAG laser (Surelite I-10 or Minilite, Continuum). A continuous-wave xenon lamp (150 W; L2274, Hamamatsu Photonics, Shizuoka, Japan) was used for a probe light source with a heat-absorption water cell, neutral density filters, and UV cutoff glass filters. The transmitted probe light was detected with a photomultiplier (R3825, Hamamatsu Photonics) coupled with a grating monochromator (f = 100 mm, 150 grooves/mm, CT10, JASCO, Tokyo, Japan). The scattering of the laser was rejected by appropriate sharp cutoff filters. The output signals from the photomultiplier were stored and averaged with an AD converter (APC-204, Autonics, Kanagawa, Japan).

RESULTS

Photovoltage generation by shR as a function of Cl^- concentrations

Fig. 1 shows the typical photovoltage generation by shR at various Cl^- concentrations ($MgCl_2$ as a salt). A laser pulse was applied at time 0. The downward signal corresponds to the negative charge movement from the extracellular side to the cytoplasmic side. The very fast positive peak (time constant $\ll$ 0.1 ms) is evident in Fig. 1 *A* (0.1 M Cl^-), and a trace of this positive signal may be seen also in Fig. 1 *B* (3 M Cl^-). This signal may correspond to the small electrogenicity during the K intermediate formation reported by Ludmann et al. (2000), but it was not taken into account in the following analyses because it was beyond our time resolution and sometimes overlapped by an electric noise caused by the laser pulse. The very slow component with positive amplitude in Fig. 1 *A*, which is also seen in the residual noise, is a baseline drift. This drift was caused by the spontaneous discharge of the membrane system and was inherent to our experimental system. This component was not taken into account, either. The rest of the signal was satisfactorily expressed as a sum of two exponential components with characteristic time constants as reported previously (Muneyuki et al., 1999). One was in the sub-millisecond range, and the other was above the millisecond range. The dashed lines in Fig. 1 are theoretical curves, and gray lines express residual noise. A single-exponential curve did not give a satisfactory fit. Here we found that the time constant for the slower process markedly increased as the Cl^- concentration increased as is particularly evident in

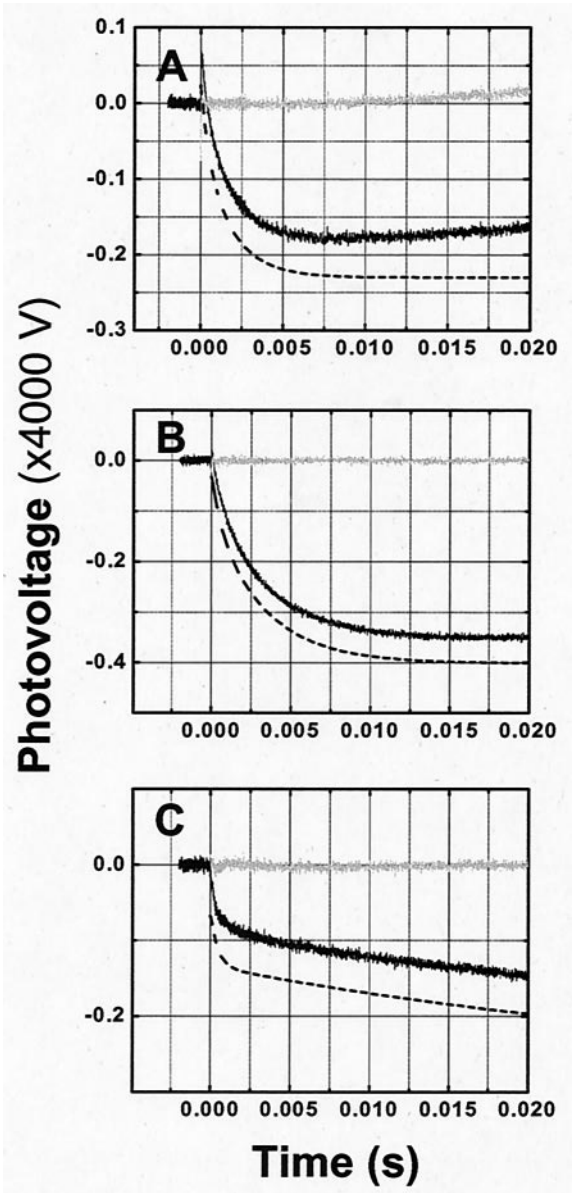

FIGURE 1 Typical photovoltage generation by shR upon laser flash. The buffer conditions were 50 mM Tris-maleate, pH 7, plus 0.05 M $MgCl_2$ (*A*), 1.5 M $MgCl_2$ (*B*), or 4.0 M $MgCl_2$ (*C*). Cl^- concentrations in *A*, *B*, and *C* were 0.1, 3, and 8 M, respectively. Dashed lines are the theoretical curves composed of two exponentials, which gave time constants and amplitudes of the fast and slow components. These parameters (time constant 1, time constant 2, amplitude 1, amplitude 2) are (0.45 ± 0.01 ms, 1.8 ± 0.0 ms, 0.07 ± 0.00, 0.18 ± 0.00), (0.61 ± 0.01 ms, 3.3 ± 0.0 ms, 0.076 ± 0.001, 0.29 ± 0.00), and (0.47 ± 0.01 ms, 36 ± 0 ms, 0.066 ± 0.000, 0.15 ± 0.00) for *A*, *B*, and *C*, respectively. These parameters are also plotted in Fig. 2, *C* and *D* (*squares*). As the theoretical curves completely overlapped the experimental data and are difficult to see, they are shifted downwards by 0.05 units. Gray lines after time 0 represent the difference between the experimental data and the theoretical curve.

Fig. 1 *C* (8 M Cl^-). On the other hand, the time constant for the fast (sub-millisecond) process showed no significant Cl^- dependence. The time constants and amplitudes of the two components are plotted against Cl^- concentration in Fig. 2, *A* and *B* ($CaCl_2$ as a salt). Data obtained with $CaCl_2$, $MgCl_2$, LiCl, and NaCl are summarized in Fig. 2, *C* and *D*. All the data indicated that the time constant for the slow process increased with the increase in Cl^- concentration and that the time constant for the fast process remained essentially the same. The slow process made up ~80% of the total amplitude. The amplitude exhibited a distorted bell-shaped Cl^- concentration dependence, consistent with our previous report (Okuno et al., 1999). The apparent increase of the photovoltage amplitude between 1 and 3 M Cl^- or a shoulder around 1 M Cl^-, which is seen in Fig. 2 *B* but not evident in Fig. 2 *D* or Fig. 3 *B*, may have arisen by some error of the measurement. In this manuscript, we will discuss the photovoltage generation above 3 M Cl^- where the changes in both photovoltage amplitude and time constant are observed.

It is well known that the halorhodopsin from *H. salinarum* is a mixture of all-*trans* and 13-*cis* retinal-containing chromophores. Therefore, it is always necessary to take the photoreaction of 13-*cis* chromophore into account. Actually, our photochemical cycle data clearly indicate that the 13-*cis* photocycle is also driven as described in the following sections. However, we can easily discriminate between the all-*trans* and 13-*cis* cycles. The latter is slower than the former, and the fraction of the latter decreases with the increase in Cl^- concentration. If such a parallel photocycle also affected to a significant extent in our photovoltage measurements, we would expect to see clear evidence of more than one time constant in the range beyond 1 ms. In this time range, however, one time constant in addition to another time constant in the sub-millisecond range was enough to describe the photovoltage data. Therefore, the contribution of the 13-*cis* photocycle to the partial charge movement in the present study seems to be very small if any. It is widely accepted that the 13-*cis* photocycle is not associated with a net charge movement.

As we applied extremely high Cl^- concentrations in this study, one may argue that the observed concentration dependence was caused by the changes in ionic strength. Indeed, it was impossible to maintain a constant ionic strength due to the limited solubility of these salts. To examine the effect of ionic strength, we added various concentrations of $(NH_4)_2SO_4$ while keeping Cl^- concentration at 1 M (Fig. 3). For comparison, the obtained parameters are shown together with those obtained using $CaCl_2$ as a salt. The time constant for the slow process increased slightly at increasing $(NH_4)_2SO_4$ concentrations, but the extent of increase was much smaller than that observed with chloride salts. The close coincidence of the data obtained using NaCl, LiCl, $CaCl_2$, and $MgCl_2$ in Fig. 2 further suggests that the observed changes in the photovoltage parameters were not caused by mere changes in ionic strength. Ca^{2+} is known to alter the properties of lipid bilayers; however, the data obtained using different salts

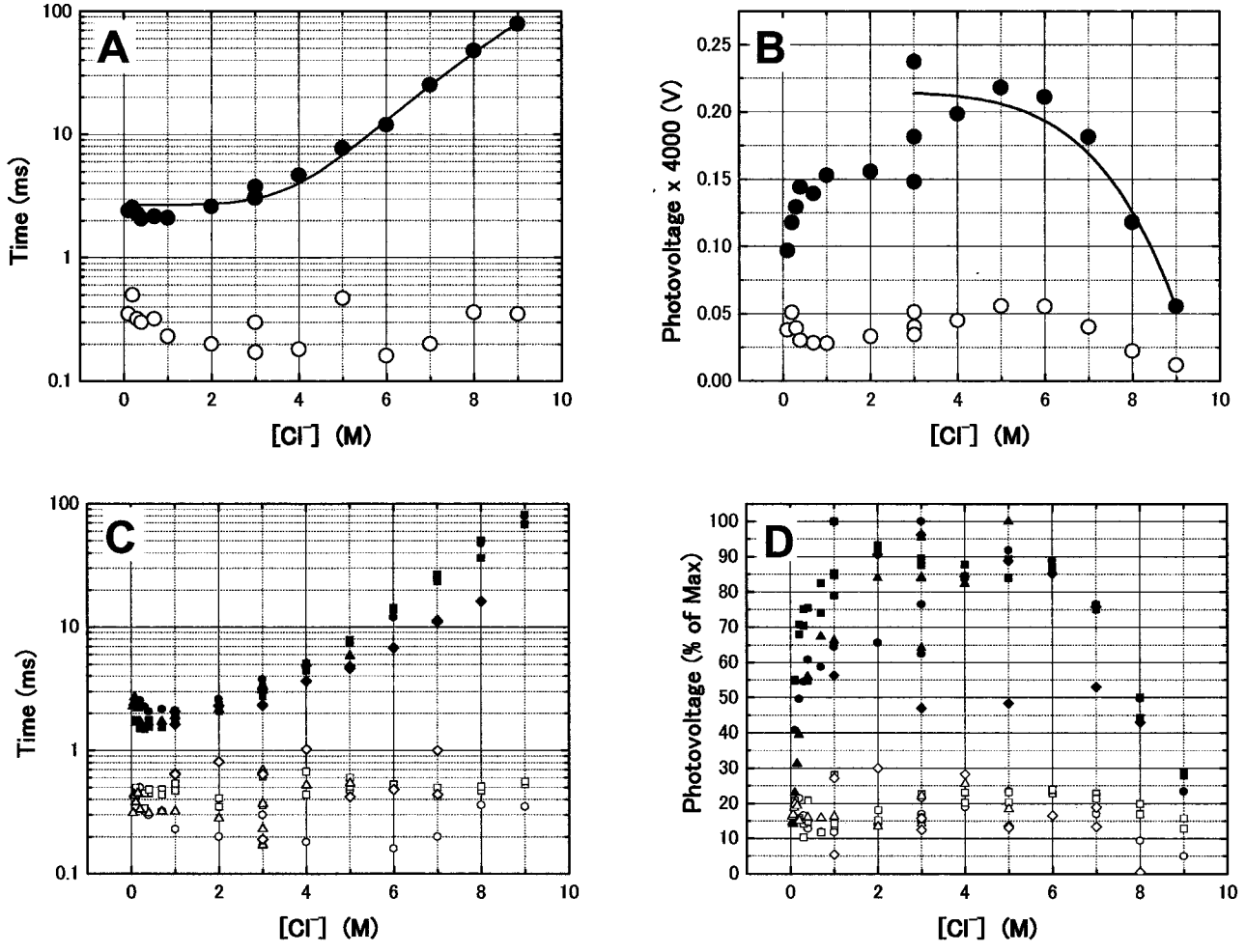

FIGURE 2 Cl^- concentration dependence of the photovoltage parameters. (*A*) Time constants obtained using $CaCl_2$: ● and ○, time constants of the slow process and the fast process, respectively. The line was drawn according to Eq. 1 with $n = 5$, $K_D = 4.6$ M, and $C = 1.24 \times 10^{-6}$. (*B*) Amplitude parameters obtained using $CaCl_2$: ● and ○, amplitudes of the slow process and the fast process, as in *A*. The line was drawn according to Eq. 3 with $n = 5$, $K_D = 4.6$ M, $C = 1.24 \times 10^{-6}$, and $\tau = 101$ ms. (*C*) Summary of the time constants obtained using $CaCl_2$ (● and ○), $MgCl_2$ (■ and □), LiCl (◆ and ◇), and NaCl (▲ and △). Filled and open symbols again correspond to the slow and fast processes, respectively. (*D*) Summary of the amplitude parameters. The symbols are the same as in *C*.

indicate that there is only a small Ca^{2+}-specific effect on the shR-overproduced membranes in which hR forms two-dimensional crystals and the lipid content is low. A small difference between LiCl and $CaCl_2$ or $MgCl_2$ is noticeable at high Cl^- concentrations. This may be attributable to the chaotropic character of Li^+ ion or may reflect some difference between monovalent and divalent cations. Although we think the latter possibility unlikely, if divalent cation were adsorbed by the surface of the membrane or film, it may attract Cl^- ions and retard the Cl^- release from hR. But the difference is relatively small, and we conclude that the effects of cation species or ionic strength on the photovoltage parameters are minor, if they exist at all. The observed change in the parameters most likely reflects the Cl^- concentration dependence of the transport process.

Photochemical cycle of shR as a function of Cl^- concentrations

Visible and infrared spectroscopic studies on shR identified the photointermediates as more or less equivalent to K (or KL), L, and O of the bR photocycle (Lanyi, 1990; Oesterhelt, 1995). Váró et al. (1995c) proposed an all-*trans* photocycle, which is coupled to Cl^- translocation, as follows:

$$HR^{h\nu} \rightarrow K \rightarrow L1 \leftrightarrow L2 \leftrightarrow N \rightarrow HR$$

The L state of shR consists of two substates, L1 and L2 (Chon et al., 1999; Váró et al., 1995c) or HR520I and HR520II (Rüdiger and Oesterhelt 1997), which seem to play a critical role in Cl^- pumping, as shown for the two M substates in proton pumping by bR (Nagel et al., 1998). We

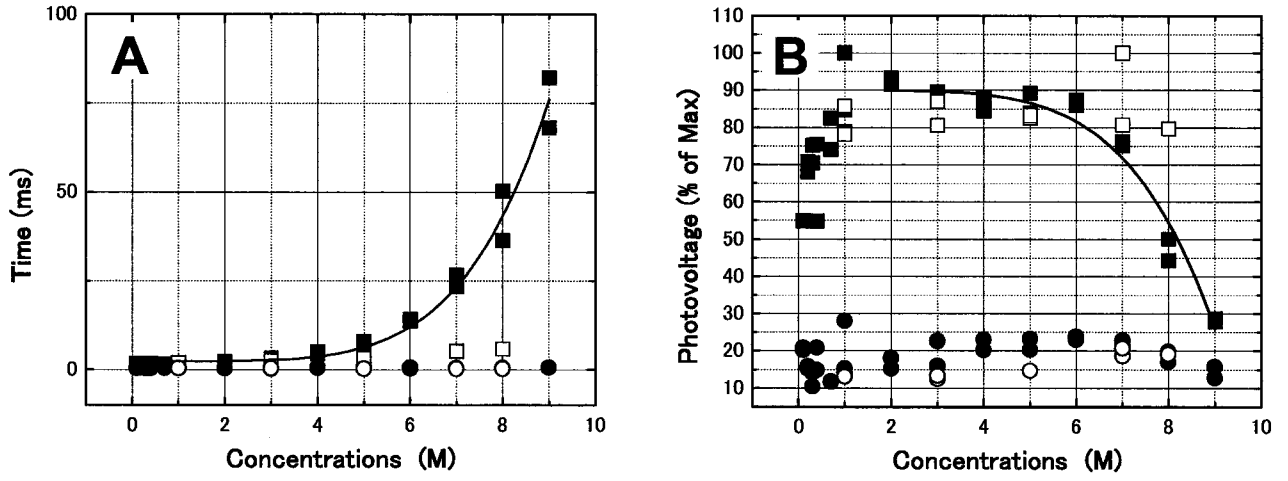

FIGURE 3 The effect of ionic strength on the photovoltage generation. To examine the effect of ionic strength, we compared the photovoltage parameters obtained in the presence of various concentrations of $MgCl_2$ (● and ■) or in the presence of 1 M NaCl plus various concentrations of $(NH_4)_2SO_4$ (○ and □). For the filled symbols, the abscissa indicates Cl^- concentration. For the open symbols where Cl^- concentration was kept at 1 M, the abscissa indicates the value of ([Cl^-] plus 2 × [SO_4^{2-}]). NaCl was used rather than $MgCl_2$ or $CaCl_2$ because some precipitation appeared when a $MgCl_2$ or $CaCl_2$ solution was mixed with the $(NH_4)_2SO_4$ solution. (*A*) The time constants. The curve was drawn to fit the filled squares according to Eq. 1 with $n = 5$, $K_D = 4.6$ M, and $C = 1.24 \times 10^{-6}$. (*B*) The amplitudes of the two exponential components are plotted against salt concentration. The line was drawn to fit the filled squares according to Eq. 3 with $n = 5$, $K_D = 4.6$ M, $C = 1.24 \times 10^{-6}$, and $\tau = 106$ ms.

previously compared the photovoltage generation and photochemical cycles of shR and phR and concluded that the major Cl^- movements in the sub-millisecond and millisecond time range correspond to N intermediate formation and decay, respectively (Muneyuki et al., 1999). This conclusion was recently confirmed by Ludmann et al. (2000), but a Cl^--concentration-dependent rate constant was not seen in the previous photochemical cycle measurement (Váró et al., 1995c). This was probably due to the limited concentration range of Cl^- examined (<2M). Here we compared the photochemical cycle with the photovoltage signal measured over a wide Cl^- concentration range.

Fig. 4 *A* shows the photochemical cycle at 3 M Cl^-. Upon excitation with a laser flash, shR showed an immediate absorbance decrease and increase at 600 and 504 nm, respectively, indicating the rapid K-to-L conversion (i.e., within 20 μs = resolution time in the present study). Váró et al. (1995c) reported that during the N formation, the amount of L remains relatively constant due to an equilibrium of the photointermediates and only the decrease of K

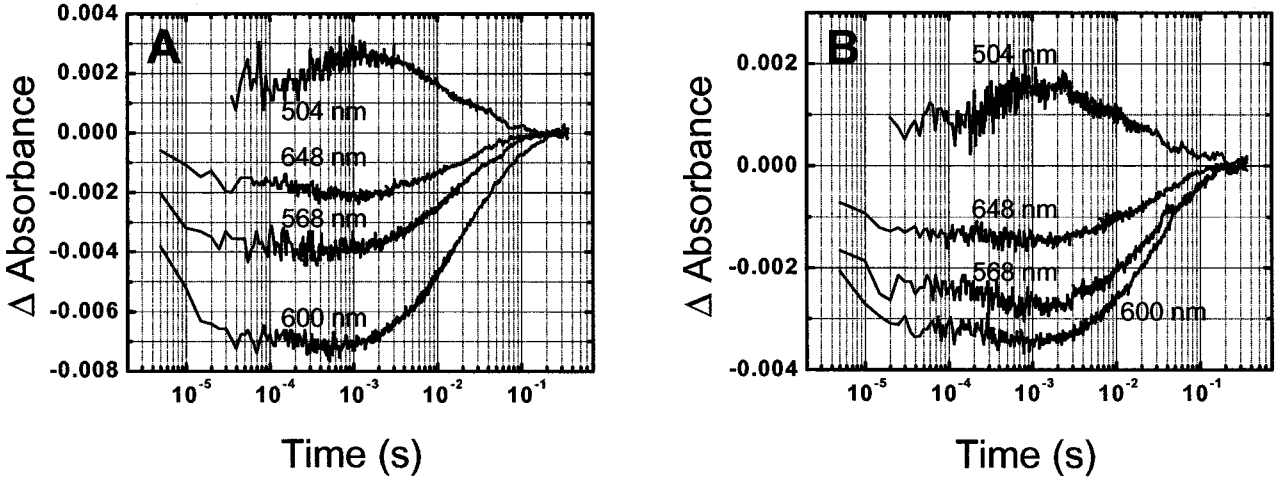

FIGURE 4 Transient absorption changes in shR upon laser flash. Absorbance changes in shR at the indicated wavelengths are shown on a logarithmic scale. (*A*) 1.5 M $CaCl_2$; (*B*) 2.5 M $CaCl_2$. Cl^- concentrations in *A* and *B* were 3 and 5 M, respectively. The difference in the magnitude of absorbance change between *A* and *B* is mostly because of the difference in sample concentration.

is spectroscopically significant. The present results are consistent with those reported. The slight absorbance decrease, which follows, at 568, 600, and 648 nm (τ = 0.25 ± 0.05 ms) and the increase at 504 nm correspond to the N formation. The following processes were analyzed as a sum of two exponents (τ = 15 ± 4 and 72 ± 16 ms). The faster and the slower processes were attributed to the cycles of an all-*trans* and a 13-*cis* pigment, respectively, because the fraction of the slower process decreased when the sample was light-adapted with a background light (λ 440 nm). Thus it was attributed to the cycle of the 13-*cis* pigment.

These assignments are consistent with the cycle of the 13-*cis* pigment being slower than that of the all-*trans* pigment (Váró et al., 1995c). Differences in the time constants between this study and Váró et al. (1995c) may originate from differences in experimental conditions.

In Fig. 4 *B*, we examined the photochemical cycle of shR at 5 M Cl^-. Although the signal-to-noise ratio was somewhat lower than that at 3 M Cl^-, it is evident that the slight decrease at 600 nm between 10^{-4} and 10^{-3} s observed in Fig. 4 *A* shifted to the right to a small extent, and judging from the change between 10^{-2} and 10^{-1} s, the regeneration of the parent state was largely retarded. The time constant of N formation at 5 M Cl^- was estimated to be 0.3 ms. The time constants for the N-to-shR conversion and the recovery of a 13-*cis* pigment were estimated to be 32 ± 5 ms and ≥140 ms, respectively. The time constant of the N decay at 5 M Cl^- increased by a factor of two compared with the time constant at 3 M Cl^-. This factor of two is in accordance with the increase in the time constant of the photovoltage generation of the slower process. Actually, the time constant of the slower photoelectrogenic process at 5 M Cl^- was 2.2 times longer than the time constant at 3 M Cl^- (an average of the data with $CaCl_2$, $MgCl_2$, NaCl, and LiCl; see Fig. 2 *C*). The fraction of the 13-*cis* cycle decreased with the increase in Cl^- concentration. For example, the absorbance change at 600 nm because of the all-*trans* cycle (τ = 16 ms) was equal to that due to the 13-*cis* cycle (τ = 74 ms) at 3 M Cl^-. On the other hand, the fraction of the all-*trans* cycle (τ = 33 ms) was nine times larger than that of the 13-*cis* cycle ($\tau \geq$ 140 ms) at 5 M Cl^-. At 7 M Cl^-, a sample suspension exhibited no signal attributed to the 13-*cis* pigment. The elongated time constant (65 ± 13 ms; data not shown) was attributed to the lifetime of N.

The measuring conditions for photovoltage signals (membranes attached to a polymer film) are different from that of optical measurements (membrane suspension). It is known from the literature that in the case of bR, data obtained with similar electric measurements and optical measurements do not agree precisely (Holz et al., 1989). These differences may be due to the difference in local concentrations of transported ions in the two experimental systems and mainly show up in the slow components of the photocycle. In our case, there was not a precise agreement between the time constants for photovoltage generation and absorbance change; however, the same time range and similar Cl^- concentration dependence strongly indicate that the two major electrogenic processes correspond to the formation and the decay of N, which is consistent with our previous conclusion (Muneyuki et al., 1999) and others (Ludmann et al., 2000). Our present results further extend the understanding that the latter process becomes significantly slower at higher Cl^- concentration, indicating this step is relevant to Cl^- release from the protein.

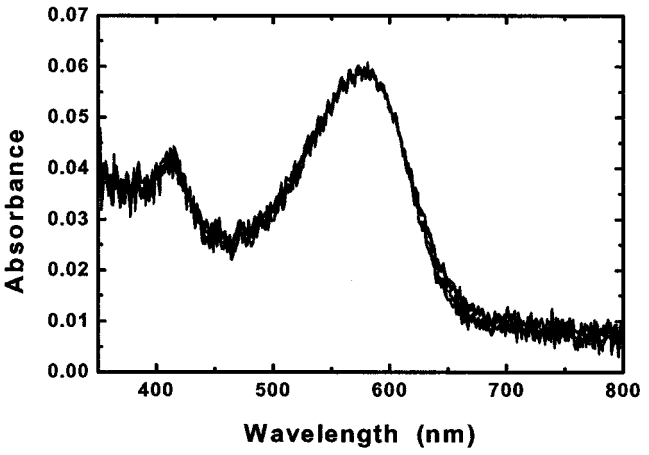

FIGURE 5 Absorption spectra of shR-overproduced membranes at various Cl^- concentrations. The spectra at 0.3, 1.0, 1.6, 3.0, 4.3, and 5.6 M Cl^- (Ca salt) are shown. They overlapped each other fairly well, as no salt concentration dependence on spectrum was observed.

In Fig. 2, the amplitude of the photovoltage decreased at high Cl^- concentration. It is possible that the decrease reflected the change in the absorption spectrum. To check this possibility, we measured the absorption spectrum of the shR membrane suspensions at various concentrations of $CaCl_2$. The spectra obtained in 0.3–5.6 M Cl^- are shown in Fig. 5. It is clear that neither spectral shape nor extinction coefficient was dependent on the Cl^- concentration over this range. At a Cl^- concentration higher than 5.6 M, we could not measure the spectra due to the turbidity. As the highest Cl^- concentration examined here did not cover the concentration range in photovoltage measurement, we cannot confidently conclude that the decrease in amplitude at extremely high Cl^- concentration was not caused by some change in absorption spectra. However, the change in the photovoltage amplitude was at least reversible, and it seems likely that the change was not due to some irreversible denaturation. In the Cl^- concentration range examined in Fig. 5, the increase in the time constant for the slow process was already prominent (Fig. 2, *A* and *C*), indicating that this increase was not due to the spectral change in shR or denaturation.

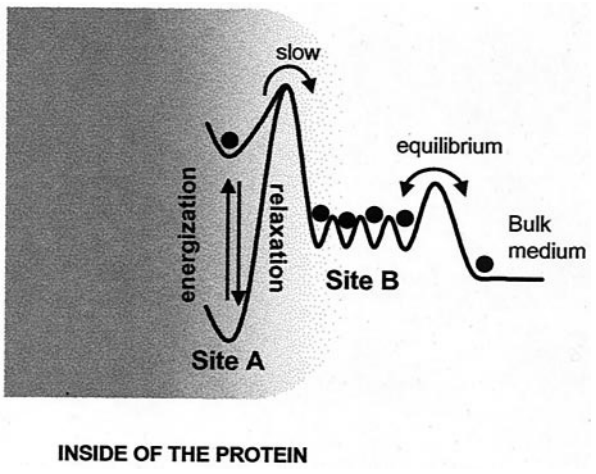

FIGURE 6 A schematic model to explain the Cl^- concentration dependence of the slow electrogenic process at high Cl^- concentrations. Upon photoexcitation, the potential of the Cl^--binding site inside of the protein (site A) is elevated (designated as energization). Then the Cl^- ion moves to a binding site near the surface, which is in equilibrium with the bulk medium (site B). As is written in the text, this site B may not be a fixed binding site. Rather, site B may correspond to some surface region (e.g., Arg-rich region of the cytoplasmic surface) where multiple Cl^- ions repulsing one another interact with this surface weakly and none of them is rigidly fixed. To express this situation, we have drawn site B as a broad trough with multiple shallow wells, but this cartoon should not be regarded as a precise description. The time constant for the Cl^- movement from site A to site B corresponds to the average waiting time before the movement. When the surface site (site B) is occupied with other Cl^- ions, the time constant increases. On the other hand, spontaneous relaxation of the potential of site A (designated as relaxation) may occur in competition with the Cl^- movement to site B. For additional explanation, see text.

Analyses of the Cl^- concentration dependence of the slow photovoltage generation

The above results on the Cl^- concentration dependence of the slower electrogenic step indicate that this step is related to Cl^- release from the protein. However, this does not necessarily imply that a Cl^- ion is directly released to the bulk medium in this step. Rather, it indicates that Cl^- moves from inside of the protein (site A in Fig. 6) to a Cl^--binding site that is in equilibrium with the bulk medium (site B in Fig. 6). (In the previous paper (Okuno et al., 1999), we proposed a model that assumed three Cl^--binding sites. They were termed sites A, B, and C. In the present study, sites A and B in Fig. 6 correspond to the sites B and C in the previous model, respectively.) site B plays a role similar to the proton release group of bR (Balashov et al., 1999). Then, in a simple case, as shown in Fig. 6, the Cl^- concentration dependence of this electrogenic process (τ) is expressed as (see Appendix for details):

$$\tau = C(K_D^n + [Cl]^n), \quad (1)$$

where C is a proportional coefficient, K_D is an apparent dissociation constant of site B that is in equilibrium with the bulk medium, and n is equivalent to the Hill coefficient. When there is no cooperativity, n equals 1. An n value greater than 1 indicates some positive cooperativity. When we fit the data with Eq. 1, an n value greater than 5 and a K_d around 4–5 M were obtained (Figs. 2 *A* and 3 *A*, solid line). (The n value between 5 and 7 gave an equally good fit to the experimental data with slightly different K_D values. As it is not our purpose to specify an exact value of n or K_D here, we simply showed the approximate range of these parameters. The lines in Figs. 2 *A* and 3 *A* are drawn using $n = 5$ and K_D of 4.6 M. The data in Figs. 2 *A* and 3 *A* may not seem to reach a saturating point, but this is because the rate constant (inverse of the time constant) is monotonously decreasing to zero. Actually, at 9 M Cl^-, the rate constant of the slower process is less than 3% of the maximum, and the present data cover a wide enough range of titration to deduce the approximate K_D. The high Hill coefficient also indicates that the data are reaching saturation.)

As Cl^- concentration increased, the time constant for the slower electrogenic process increased and concomitantly its amplitude decreased. The apparent Cl^- concentration that gives half-maximal photovoltage amplitude in the decreasing phase (~8 M in Figs. 2, *B* and *D*, and 3 *B*) do not agree with the above obtained K_D of site B (4–5 M). This decrease in the amplitude requires some explanation. The amplitude of the photovoltage results from the total charge moved from site A to site B (Fig. 6). The time constant reflects the average waiting time for the Cl^- ion movement. Then, once the photocycle has started, the amplitude should not depend on the Cl^- concentration even if the accompanying time constant becomes significantly longer. This is because once the Cl^- bound at site A is energized, after all, it may find a chance to move to site B, which is occasionally empty because of the equilibrium with the external medium. Nevertheless, the photovoltage amplitude decreased at increasing Cl^- concentrations. There may be at least three possible reasons for the observed amplitude decrease. The first formal possibility is that the decrease is only an artifact, caused by the system discharge inherent to our experimental setup. This possibility seems to contribute little, if at all, to the observed decrease in the amplitude because the time constant for our present system discharge (~500 ms; see also Fig. 1 *A*) is sufficiently longer than the time constant for the electrogenic process. The second possibility is that at extremely high Cl^- concentration, some decrease in the molar extinction coefficient of shR at the excitation wavelength may occur. This possibility can also be excluded because there is no change in the spectrum of shR at least up to 5.6 M Cl^-, as shown in Fig. 5. The third possibility is related to the Cl^--translocating mechanism. When a photon is absorbed and Cl^- ion moves, the potential for the Cl^- ion at site A is elevated (energization in Fig. 6). (This is a rather simplified picture. The energization here actually may contain several events leading up to the L intermediate formation as suggested by a recent Fourier transform infrared

study (Hutson et al., 2001).) The energy stored in this state is usually liberated by the Cl^- movement down the potential to site B. However, when this movement cannot take place because of the occupation of site B by other Cl^- ion(s) from the bulk medium, the stored energy may be liberated by a spontaneous relaxation of the protein (relaxation in Fig. 6). This process should be strictly prohibited to achieve the high efficiency for ion translocation. Under extreme conditions, such as those employed in the present study, such a process may compete with the normal reaction pathway. In this case, the origin of the apparent Cl^- concentration for the half-maximal photovoltage amplitude is different from the K_D of site B, and they do not necessarily agree with each other. When we assume the competition between the transport and spontaneous relaxation, a linear relationship between the time constant and amplitude of photovoltage generation is expected (see Appendix for details):

$$A(\infty) = Eo(1 - k_r\tau), \quad (2)$$

Here, $A(\infty)$ and τ are the total amplitude and time constant for the photovoltage, and k_r is a rate constant for the spontaneous relaxation. *Eo* is the total charge movement in the absence of spontaneous relaxation. Note that this relationship is valid only where photovoltage amplitude is limited by the occupation of site B by Cl^- and spontaneous relaxation (3 M Cl^- in the present study). Between 0 and 3 M Cl^-, other factors such as Cl^- binding to an extracellular surface site, may become a limiting factor to the photovoltage amplitude. Combined with Eq. 1, the Cl^- concentration dependency of the photovoltage amplitude at the high Cl^- concentration range is given by (see Appendix for details):

$$A(\infty) = Eo(1 - k_r \times C(K_D^n + [Cl]^n)) \quad (3)$$

When we plotted the data according to Eq. 2, a linear relationship was indeed observed (Fig. 7 *inset*). From the plot, the rate of spontaneous relaxation was calculated to be 9.7 s^{-1}, and the averaged lifetime of the energized state was estimated to be 103 ms. The averaged values ± SE of four independent experiments were 10.1 ± 0.4 s^{-1} (rate constant, k_r) and 98.9 ± 3.6 ms (lifetime). The Cl^- concentration dependency of the photovoltage amplitude was reproduced by Eq. 3 fairly well as seen in Figs. 2 *B* and 3 *B*. Although the first two possibilities, which we consider remote, may contribute to some degree to the decrease in the photovoltage amplitude, they would not affect the validity of the present conclusion that the energized state has a very long lifetime.

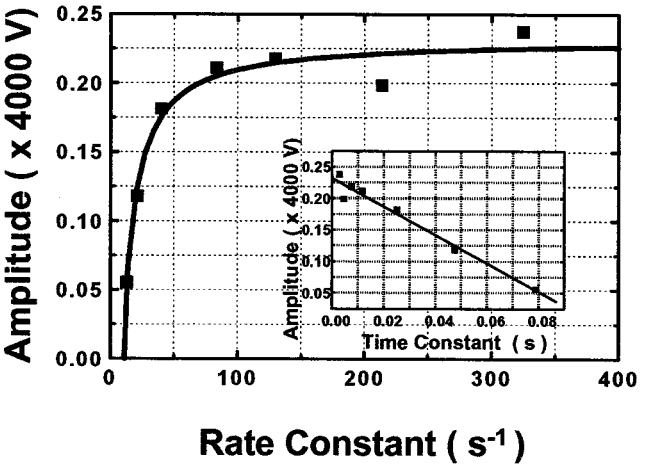

FIGURE 7 Relationship between the photovoltage amplitude and rate of charge movement at high Cl^- concentrations. The amplitude of photovoltage, which corresponds to $A(\infty)$ in Eq. 2, was plotted against the rate of charge movement. The rate of charge movement is the inverse of the time constant ($1/\tau$). Data are taken from Fig. 2, *A* and *B*. (*Inset*) The amplitude ($A(\infty)$) versus time constant (τ). The slope of this linear plot gives the rate constant for spontaneous relaxation (k_r). See text and Appendix for additional details.

DISCUSSION

Previously, we detected two major electrogenic steps during the photocycle of hR and proposed that they corresponded to the N formation and decay (Muneyuki et al., 1999). This conclusion was recently confirmed by others (Ludmann et al., 2000). However, it was not clear whether the two steps corresponded to Cl^- uptake from the medium, Cl^- release to the medium, or Cl^- translocation within the protein molecule. To gain insights into these points, it is essential to examine the Cl^- concentration dependence of these steps. Up to now, several groups have reported the presence or absence of the Cl^- dependence of the photochemical rate constants. Zimányi and Lanyi (1989) found that the rate constant for the O-to-L back transition is proportional to the Cl^- concentration and proposed that the O formation corresponds to Cl^- release. A resonance Raman study also supported Cl^- release during the O intermediate formation (Ames et al., 1992). Váró et al. did not find a Cl^--dependent rate constant in shR photocycle (Váró et al. (1995c) but found Cl^--dependent rate constants for the phR photocycle and concluded that the N decay (i.e., the O formation) corresponds to Cl^- release and that Cl^- uptake takes place during O intermediate decay for phR (Váró et al., 1995a,b). In the present study, we examined the photoelectrogenic response of shR over a wide Cl^- concentration range. It was clear that, of the two major electrogenic processes, the slower one, which we previously assigned as the N decay, decelerates at higher Cl^- concentrations. Thus, this step is highly likely to be related to Cl^- release from the protein. Our photochemical cycle data also support this contention. Some of the authors did not include N in their photocycle model of halorhodopsin (Ames et al., 1992; Zimányi et al., 1989; Zimányi and Lanyi, 1989), and our conclusion apparently looks contradictory to theirs. However, if we regard the N decay as the O formation, our conclusion that the N

decay is related to Cl^- release becomes consistent with those of most of the others. We found that the fast electrogenic process did not show significant Cl^- dependence. The present results suggest that this process, corresponding to N formation (i.e., L decay), is a Cl^- movement inside of the protein.

It seems that the photocycle starts from the Cl^--bound state so that Cl^- reuptake occurs during the recovery of the parent state. We could not actually detect an electrogenic step that is significantly accelerated at increasing Cl^- concentrations. This could be because of the limitations of our experimental system, which cannot follow a very slow electrogenic process because of the system discharge (time constant $>$ 500 ms). However, according to Ludmann et al. (2000), there is little electrogenicity after the N decay. This may be because the Cl^- uptake may occur very slowly or the electric distance of the uptake pathway is rather short or both. Actually, the structure of the extracellular half of shR is more hydrophilic than the cytoplasmic half, as is evident from the fact that more water molecules are seen in the extracellular half of the crystal structure (Kolbe et al., 2000). Such a structural features make the electric distance of the Cl^- uptake pathway shorter than the physical distance.

Previously, we suggested that Cl^- binding to the cytoplasmic surface site (site B in Fig. 6) is very weak and highly cooperative (Okuno et al., 1999). The present analysis of the Cl^- concentration dependency of the slower electrogenic step revealed a highly cooperative ($n \geq 5$) and weak binding (apparent $K_D \sim 5$ M; Figs. 2 *A* and 3 *A*, solid line). These values are a little smaller than those reported previously ($n = 8$; $K_D = 7.5$ M (Okuno et al., 1999)). In the previous study, the photocurrent was induced by continuous illumination and the results contained the contribution of multiple steps. In view of the different measurement system, the present data are in good accordance with the previous one. The origin of the apparent cooperative and low-affinity binding is not clear yet. Actually, site B may not be a well defined binding site in a usual sense. According to the crystal structure, Arg258, Arg52, Arg55, Arg58, and Arg60 form a positively charged patch on the cytoplasmic surface. However, no Cl^- binding was observed in this region (Kolbe et al., 2000). It is plausible that multiple Cl^- ions repulsing one another interact with this surface weakly and none of them is rigidly fixed. It could be a shielding effect of the charges on the surface of the membrane that prevents the Cl^- movement from site A to site B in Fig. 6.

The Cl^- concentration dependence of the photovoltage amplitude suggested an interesting aspect of the energized state of shR. In general, any energy-transducing protein has at least two states, the energized state and the relaxed state. When the two states provide different asymmetric environments for the load (i.e., transported ions for ion pumps or movable parts of motor proteins), the active motion of the load is induced by nonequilibrium transitions between the two states (Prost et al., 1994; Astumian and Bier 1996; Muneyuki and Fukami 2000). In the case of hR, it is obvious that light absorption is the step of energization. To achieve active transport, the energy must be used to elevate the potential of a bound Cl^-, and Cl^- movement down the potential gradient liberates part of the stored energy (Fig. 6). (Alternatively, in a general case, the energy may be used to switch the accessibility of the transported ion rather than elevation of the potential of a bound ion.) The direction of the Cl^- movement may be determined by some gating mechanism or by Cl^--binding site occupancy, as previously proposed (Muneyuki et al., 1999; Okuno et al., 1999). Usually, the stored energy is not to be liberated without Cl^- movement. However, the energized state must be inherently unstable, and when Cl^- movement is retarded under some extreme conditions such as those used in the present study, spontaneous relaxation without Cl^- movement may compete with the normal transporting process. In the present study, the relationship between the amplitude and time constant of photovoltage generation was analyzed according to the above scenario. The analysis gave a lower limit for the lifetime of the energized state, which was quite long (100 ms). Although spontaneous relaxation is not impossible, it seems strictly restricted, and energy dissipation without Cl^- transport is prevented under physiological conditions. The mechanism of energy storage within a protein structure for such a long time is very important for efficient energy transduction. In the present study, we examined the photovoltage generation only at room temperature because of technical limitations, but it would be interesting to examine the temperature effects. Depending on the rigidity of the protein, which prevents spontaneous relaxation and the mobility of Cl^- within the protein, the relationship between photovoltage amplitude and time constant at high Cl^- concentration would be different at different temperatures. Such information will be important, and it will be fascinating to understand the mechanism of energy storage for shR to determine whether other energy-transducing proteins share a similar mechanism.

APPENDIX

Explanation for Eq. 1

The Cl^- movement from site A to site B (Fig. 6) may be described as follows:

$$A \cdot Cl^- + B \rightarrow A + B \cdot Cl^-$$

Here, A and B stand for the Cl^--free form of site A and site B, and A·Cl^- and B·Cl^- stand for the Cl^--bound form of site A and site B. Thus, the rate of Cl^- transfer from site A to site B is proportional to [B].

On the other hand, if site B is in equilibrium with the bulk medium with an apparent dissociation constant of K_D as described below:

$$B + nCl^- \leftrightarrow B \cdot Cl_n^-,$$

then $[B]$ is described as in Eq. 4:

$$K_D^n = \frac{[B][Cl^-]^n}{[B \cdot Cl_n^-]} \quad (4)$$

$$[B] = \frac{K_D^n [B_t]}{K_D^n + [Cl^-]^n} \quad (5)$$

$[B_t]$ is the total concentration of site B. Here we assumed highly cooperative binding (Hill coefficient = n) at site B.

As the numerator in Eq. 5 can be regarded as a constant, the rate of Cl^- transfer is proportional to $1/(K_D^n + [Cl^-]^n)$, which means the time constant equals $C(K_D^n + [Cl^-]^n)$. Here, C is a proportional coefficient.

Explanation for Eqs. 2 and 3

From the energized state of the Cl^--bound site A, we assume that the Cl^- transfer to site B (rate constant = k_t) and spontaneous relaxation without Cl^- transfer (rate constant = k_r) occur in parallel (see Fig. 6). Then, the total charge movement ($A(\infty)$) is proportional to $k_t/(k_t + k_r)$:

$$A(\infty) = Eo \frac{k_t}{k_t + k_r}, \quad (6)$$

where Eo is a proportional coefficient.

The observed lifetime of the energized form of site A is $(k_r + k_t)^{-1}$ because of the competition between the Cl^- transfer and the relaxation. Therefore, the total charge movement (photovoltage amplitude) is described as follows:

$$A(\infty) = Eo \frac{k_t}{k_t + k_r} = Eo\left(1 - \frac{k_r}{k_t + k_r}\right) = Eo(1 - k_r \times \tau) \quad (7)$$

According to Eq. 7, the plot of the photovoltage amplitude against the photovoltage time constant gives a linear curve, the slope of which is proportional to k_r. Note that the derivation of Eq. 7 and k_r is independent of the Cl^- concentration dependency of the τ or k_t.

When τ is given as in the explanation for Eq. 1, the Cl^- concentration dependency of the photovoltage amplitude will become:

$$A(\infty) = Eo(1 - k_r \cdot \tau) = Eo(1 - k_r C(K_D^n + [Cl]^n)) \quad (8)$$

This Eq. 8 was used to draw the theoretical lines in Figs. 2 *B* and 3 *B*.

Strictly speaking, the effect of spontaneous relaxation (k_r) should be included in the analysis of K_D and n in Eqs. 4 and 5; however, when this effect is taken into account, the K_D and n values do not change significantly. For example, with a k_r of 10 s^{-1}, K_D and n of 4.0 M and 5, 4.5 M and 6, or 4.8 M and 7 gave equally good fits to Fig. 2 *A*.

We thank K. Morizumi, S. Nishino, and T. Ohtaki (Toray Industries) for Lumirror, R. Needleman (Wayne State University) for the shR overproducing strain and its membranes, and Dr. Jeanne Hardy for critical reading of the manuscript.

This work was supported in part by Grants-in-Aid for Scientific Research on Priority Areas (12030210 to E.M.), and for Scientific Research (C) (11680653 to E.M.) from the Ministry of Education, Science, Sports, and Culture of Japan. This work was also supported in part by Molecular Sensors for Aero-Thermodynamic Research (MOSAIC), the Special Coordination Funds of Science and Technology Agency (to H.O.) and Scientific Research (11226101 to H.O.) from the Ministry of Education, Science, Sports, and Culture of Japan.

REFERENCES

Ames, J. B., J. Raap, J. Lugtenburg, and R. A. Mathies. 1992. Resonance Raman study of halorhodopsin photocycle kinetics, chromophore structure, and chloride-pumping mechanism. *Biochemistry.* 31:12546–12554.

Astumian, R. D., and M. Bier. 1996. Mechanochemical coupling of the motion of molecular motors to ATP hydrolysis. *Biophys. J.* 70:637–653.

Balashov, S. P., M. Lu, E. S. Imasheva, R. Govindjee, T. G. Ebrey, B. Othersen III, Y. Chen, R. K. Crouch, and D. R. Menick. 1999. The proton release group of bacteriorhodopsin controls the rate of the final step of its photocycle at low pH. *Biochemistry.* 38:2026–2039.

Chon, Y.-S., H. Kandori, J. Sasaki, J. K. Lanyi, R. Needleman, and A. Maeda. 1999. Existence of two L photointermediates of halorhodopsin from *Halobacterium salinarium*, differing in their protein and water FTIR bands. *Biochemistry.* 38:9449–9455.

Holz, M., L. A. Drachev, T. Mogi, H. Otto, A. D. Kaulen, M. P. Heyn, V. P. Skulachev, and H. G. Khorana. 1989. Replacement of aspartic acid-96 by asparagine in bacteriorhodopsin slows both the decay of the M intermediate and the associated proton movement. *Proc. Natl. Acad. Sci. U.S.A.* 86:2167–2171.

Hutson, M. S., S. V. Shilov, R. Krebs, and M. S. Braiman. 2001. Halide dependence of the halorhodopsin photocycle as measured by time-resolved infrared spectra. *Biophys. J.* 80:1452–1465.

Ihara, K., T. Umemura, I. Katagiri, T. Kitajima-Ihara, Y. Sugiyama, Y. Kimura, and Y. Mukohata. 1999. Evolution of the archaeal rhodopsins: evolution rate changes by gene duplication and functional differentiation. *J. Mol. Biol.* 285:163–174.

Kalaidzidis, I. V., Y. L. Kalaidzidis, and A. D. Kaulen. 1998. Flash-induced voltage changes in halorhodopsin from *Natronobacterium pharaonis. FEBS Lett.* 427:59–63.

Kolbe, M., H. Besir, L. O. Essen, and D. Oesterhelt. 2000. Structure of the light-driven chloride pump halorhodopsin at 1.8 Å resolution. *Science.* 288:1390–1396.

Lanyi, J. K. 1990. Halorhodopsin, a light-driven electrogenic chloride-transport system. *Physiol. Rev.* 70:319–330.

Ludmann, K.,G. Ibron, J. K. Lanyi, and G. Váró. 2000. Charge motions during the photocycle of *pharaonis* halorhodopsin. *Biophys. J.* 78: 959–966.

Muneyuki, E., and T. A. Fukami. 2000. Properties of the stochastic energization-relaxation channel model for vectorial ion transport. *Biophys. J.* 78:1166–1175.

Muneyuki, E., D. Okuno, M. Yoshida, A. Ikai, and H. Arakawa. 1998. A new system for the measurement of electrogenicity produced by ion pumps using a thin polymer film: examination of wild type bacteriorhodopsin and the D96N mutant over a wide pH range. *FEBS Lett.* 427: 109–114.

Muneyuki, E., Shibazaki, C., Ohtani, H., Okuno, D., Asaumiumi, M., and T. Mogi. 1999. Time-resolved measurements of photovoltage generation by bacteriorhodopsin and halorhodopsin adsorbed on a thin polymer film. *J. Biochem.* 125:270–276.

Nagel, G., B. Kelety, B. Mockel, G. Buldt, and E. Bamberg. 1998. Voltage dependence of proton pumping by bacteriorhodopsin is regulated by the voltage-sensitive ratio of M1 to M2. *Biophys. J.* 74:403–412.

Oesterhelt, D. 1995. Structure and function of halorhodopsin. *Israel J. Chem.* 35:475–494.

Oesterhelt, D., and W. Stoeckenius. 1974. Isolation of the cell membrane of *Halobacterium halobium* and its fractionation into red and purple membrane. *Methods Enzymol.* 31:667–678.

Ohtani, H., S. Naramoto, and N. Yamamoto. 1994. Laser photolysis of the purple membrane of *Halobacterium halobium* in the photostationary

state: the photobranching process from the O640 intermediate. *Photochem. Photobiol.* 60:394–398.

Okuno, D., M. Asaumi, and E. Muneyuki. 1999. Chloride concentration dependency of the electrogenic activity of halorhodopsin. *Biochemistry.* 38:5422–5429.

Otomo, J., H. Tomioka, and H. Sasabe. 1992. Properties and primary structure of a new halorhodopsin from halobacterial strain *mex*. *Biochim. Biophys. Acta.* 1112:7–13.

Prost, J., J.-F. Chauwin, P. Peliti, and A. Ajdari. 1994. Asymmetric pumping of particles. *Phys. Rev. Lett.* 72:2652–2655.

Rüdiger, M., and D. Oesterhelt. 1997. Specific arginine and threonine residues control anion binding and transport in the light-driven chloride pump halorhodopsin. *EMBO J.* 16:3813–3821.

Soppa, J., J. Duschl, and D. Oesterhelt. 1993. Bacterioopsin, haloopsin, and sensory opsin I of the halobacterial isolate *Halobacterium* sp. strain SG1: three new members of a growing family. *J. Bacteriol.* 175: 2720–2726.

Stoeckenius, W. 1999. Bacterial rhodopsins: evolution of a mechanistic model for the ion pumps. *Protein Sci.* 8:447–459.

Váró, G., L. S. Brown, J. Sasaki, H. Kandori, A. Maeda, R. Needleman, and J. K. Lanyi. 1995a. Light-driven chloride ion transport by halorhodopsin from *Natronobacterium pharaonis*. I. The photochemical cycle. *Biochemistry.* 34:14490–14499.

Váró, G., R. Needleman, and J. K. Lanyi. 1995b. Light-driven chloride ion transport by halorhodopsin from *Natronobacterium pharaonis*. II. Chloride release and uptake, protein conformation change, and thermodynamics. *Biochemistry.* 34:14500–14507.

Váró, G., L. Zimányi, X. Fan, L. Sun, R. Needleman, and J. K. Lanyi. 1995c. Photocycle of halorhodopsin from *Halobacterium salinarium. Biophys. J.* 68:2062–2072.

Zimányi, L., L. Keszthelyi, and J. K. Lanyi. 1989. Transient spectroscopy of bacterial rhodopsins with an optical multichannel analyzer. I. Comparison of the photocycles of bacteriorhodopsin and halorhodopsin. *Biochemistry.* 28:5165–5172.

Zimányi, L., and J. K. Lanyi. 1989. Transient spectroscopy of bacterial rhodopsins with an optical multichannel analyzer. II. Effects of anions on the halorhodopsin photocycle. *Biochemistry.* 28:5172–5178.